To be submitted to 1997 IEEE Int. Conf. on Robotics and Automation

# Pulling Motion Based Tactile Sensing for Concave Surface

Makoto Kaneko, Mitsuru Higashimori *and* Toshio Tsuji

Industrial and Systems Engineering,
Hiroshima University,
Kagamiyama, Higashi-Hiroshima, 739, Japan

*Abstract*— **An algorithm for detecting the shape of 2D concave surface by utilizing a tactile probe is proposed. Pulling a tactile probe whose tip lies on an object's surface can be easily achieved, while pushing it is more difficult due to stick-slip or blocking up with irregular surface. To cope with the difficulty of pushing motion on a frictional surface, the proposed sensing algorithm makes use of the pulling motion of tactile probe from a local concave point to an outer direction. The algorithm is composed of three phases, local concave point search, tracing motion planning, and infinite loop escape. The proposed algorithm runs until the tactile probe detects every surface which it can reach and touch. We show some computer simulations and experimental results obtained along the proposed algorithm.**

*Keywords*— **Tactile Sensing, Concave Surface, Compliant Motion, Pulling-Motion Based Sensing**

## I. Introduction

A robotic system often requires to know the local (or full) shape of object before grasping it, especially for approaching an unknown one. An obvious solution is to utilize a vision system which enables us to obtain the global information of object quickly. By applying an appropriate procedure for the visual data taken into a computer through a camera, the robot system can recognize the shape of object. If the scene includes ambiguity or lighting condition is not good enough, however, this approach easily fails.

Another solution for detecting the object shape is to utilize a tactile sensor, which is comparatively low-cost and enables us to get the shape information through the direct touch even in visually occluded areas. Because of the nature of direct touch, tactile sensing can provide not only the shape of object but also the local impedance of object.

This paper focuses on the shape detection of 2D surface by utilizing a tactile probe which can detect any contact point between it and environment. One emphasis of our research is to study how the probe motion should be planned for the object including concave surface. As well known, pushing a probe whose tip lies on an object's surface is not easily achieved due to appearance of the stick-slip or blocking brought by a small irregularity on the surface, while pulling it can be done more easily even under the same constraint. Considering this fact, we propose the pulling motion based algorithm where no pushing motion is necessary. If the environment's surface is unknown, however, whether the resulting motion becomes pulling or pushing strongly depends on the surface geometry and on the direction of the motion imparted to the tactile probe. In case that the sensing motion starts from an arbitrary point on the surface, pulling and pushing motions are expected for outer and inner directions, respectively, as shown in Fig.1(a). If we can choose the local concave point as a starting one, however, we can expect pulling motions for both directions, as shown in Fig.1(b). In order to utilize this advantage, the algorithm first searches the local concave point by applying the bisection method (*local concave point search*). The tactile probe is then pulled from a local concave point to outer directions while keeping the tip of probe in contact with the environment (*tracing motion planning*). There might be a failure mode in which the sensing motion results in repeating mode without finding any new contact

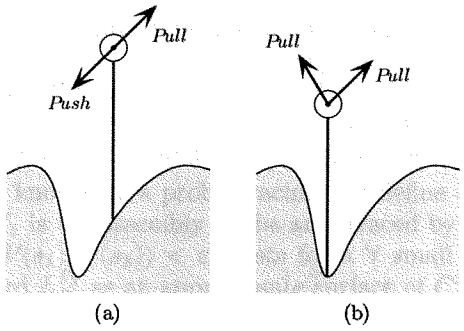


Fig. 1. Pulling and pushing motions.

point. To emerge from such an infinite loop, we prepare *infinite loop escape* by which the tactile probe can always find a new contact point if it exists. We show that the proposed algorithm can continue to run till the tactile probe detects every surface which it can reach and touch. Also, we show some computer simulation and experimental results obtained along the proposed algorithm.

## II. Related Work

There are a number of works discussing tactile and haptic perception linked with multi-fingered dexterous hands [1]–[10]. Dario and Buttazzo [1], Fearing [2], and Maekawa et. al. [3] have succeeded in obtaining some good reconstructed surfaces using the fingertip tactile sensor. As a new utilization of force/torque sensors, Salisbury [4] pointed out that force/torque information makes it possible to estimate contact location as well as contact force. Based on this idea, Brock and Chui [5] have designed a miniatured fingertip tactile sensor and showed a sensing result for a part of sphere. Kaneko and Honkawa [6] proposed an active sensing technique by using joint compliant motion, where the object shape is evaluated from the trajectory of the link posture when imparting an angular displacement to the position-controlled joint. Bays [10] proposed a simple multi-fingered surface exploration procedure, in which only the normal direction of the force sensor information is utilized for estimating the surface parameter. Caselli et. al. [11] proposed an efficient technique for recognizing convex object from tactile sensing. They developed internal and external volumetric approximation of the unknown objects and exploited an effective feature selection strategy along with early pruning of incompatible objects to improve recognition performance. On the other hand, algorithms for tactile sensing have also been reported. Gaston and Lozano-Perez [12] and Grimson and Lozano-Perez [13] discussed object recognition and localization through tactile information under the assumption that the robot possesses the object models. Cole and Yap [14] have addressed "Shape from probing" problem, where they discussed how many probes are necessary and sufficient for determining the shape and position of a polygon. They showed $3n-1$ probes are necessary and $3n$ are sufficient for any $n$-gon, where $n$ is the number of probes. Most of these works [1]–[9], [11]–[14], however, deal with convex objects only and never discuss concave ones.

As far as we know, there are only a few papers [15]–[19] addressing tactile sensing for concave objects. Russell [15] measured the concave bowl of a teaspoon by utilizing a whisker type tactile sensor. By applying the contact point sensing based on force/torque information [4], Tsujimura and Yabuta [16] succeeded in reconstructing a telephone receiver partly involving a concave shape. Roberts [17] discussed the strategy for determining the active sensing motion for the given set of convex and concave polyhedral model objects. Chen, Rink and Zhang [18] introduced an active tactile sensing strategy to obtain local object shape, in which they showed how to find the contact frame and the local surface parameters in the contact frame. In these works, they picked up extremely simple concave objects as test examples but included no precise discussion on the inherent sensing algorithm for concave objects.

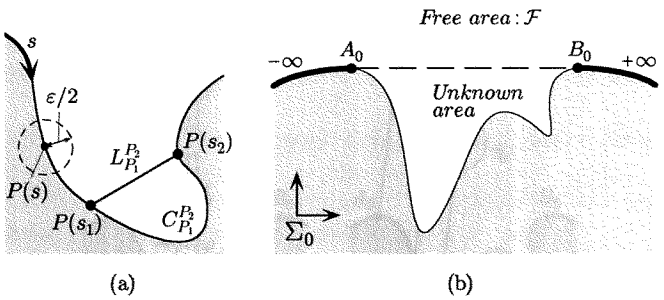


Fig. 2. Definition of symbols and problem notation.

## III. Problem Formulation

### A. Preliminary definitions

Let $P(s)$ (or simply $P$) be a point on the environment's surface, where $s$ is the coordinate along the surface as shown in Fig.2(a). We define $Dist(P(s_1), P(s_2))$, $C_{P_1}^{P_2}$ and $L_{P_1}^{P_2}$ as the distance, the environment's contour, and the line segment between $P(s_1)$ and $P(s_2)$, respectively. When $C_{P_1}^{P_2}$ becomes known by a probe tracing, we define $C_{P_1}^{P_2} \in W_1$, where $W_1$ is the assembly of the area traced by the probe. If $Dist(P(s_1), P(s_2)) < \varepsilon$ exists for a $\forall$ small $\varepsilon > 0$, we can regard $L_{P_1}^{P_2}$ as an approximate surface of $C_{P_1}^{P_2}$, and define $C_{P_1}^{P_2} \in W_2$, where $W_2$ is the assembly of approximately detected area by straight-line approximation. When the tactile probe recognizes the particular area between $P(s_1)$ and $P(s_2)$ where it can not reach and touch physically, we define the area as the non-reachable area and describe by $C_{P_1}^{P_2} \in W_3$, where $W_3$ is the assembly of the non-reachable area verified by a probing motion. For every concave object (or environment), we can make an equivalent convex shape by connecting common tangential lines. The outside of the equivalent convex is defined as the free area $\mathcal{F}$ as shown in Fig.2(b) where it is guaranteed that there is no object (or environment). We also define $Area(\mathcal{G})$ as the area of $\mathcal{G}$.

### B. Main assumptions

Distributed sensing elements cover all over the tactile probe. The probe has negligible thickness and connected with the end-joint of a robot arm having sufficient degrees of freedom so that the probe can take arbitrary position and posture in 2D plane. The arm is assumed to have a joint torque and a joint position sensors in each joint. The probe is long enough to ensure that the end-joint of the arm always exists in the free area $\mathcal{F}$, which enables us to neglect any geometrical constraint coming from the robot arm and to focus on the probe motion. The probe is sufficiently stiff to avoid bending. In order to avoid complicated discussion, we give the following assumption on the shape of environment. Consider a small circle whose center and radius are given by $P(s)$ and $\varepsilon/2$, respectively, as shown in

Fig.2(a). We also assume that there always are only two intersection points between the circle and the environment for an arbitrary $s \in [-\infty, +\infty]$. This assumption provides a valid reason for approximating the environment's contour as the straight-lined one, namely, $C_s^{s+\varepsilon} \cong L_s^{s+\varepsilon}$. We also assume that there exists only one object (or environment).

### C. Problem formulation

**Problem formulation :** *Given* $C_{P(-\infty)}^{A_0} \in W$ *and* $C_{B_0}^{P(+\infty)} \in W$, *construct an algorithm such that* $C_{A_0}^{B_0} \in W$ *is achieved under the assumption in III-B, where* $W = \cup_{i=1}^{3} W_i$.

This problem can be understood more intuitively by Fig.2(b) where $\Sigma_0$ is the absolute coordinate system.

## IV. Pulling Motion Based Sensing

### A. Outline of the algorithm

We explain the main part of the algorithm briefly so that we can understand the outline of the sensing algorithm. Fig.3 shows an example explaining the sensing algorithm. The probe is first inserted from an arbitrary point in the free area $\mathcal{F}$ toward the unknown area until the tip makes contact with the environment. By monitoring the torque sensor output, it is checked whether a clockwise (or counter clockwise) rotation of the probe is possible or not. After checking such a geometrical condition, the probe is rotated in the direction of rotation free till it again makes contact as shown by the dotted line in Fig.3(a), where $\varphi$ is the rotational angle. Choosing the equally divided direction $\varphi/2$, we again insert the probe till it makes contact with the environment. By repeating this procedure, the tip can finally reach the local concave point, where the probe loses any rotational degree of freedom (*local concave point search*). Then, the probe is moved from the local concave point to the outer direction, while maintaining constant torque control for the last joint, where a clockwise torque is applied during the prove motion from $D_0$ to $A_0$ and a counter clockwise torque is imparted during the prove motion from $D_0$ to $B_0$. Fig.3(b) and (c) show two examples of tracing motion. By imparting the torque depending on the direction of tracing motion, it is ensured that the probe tip makes contact with the environment if the surface is smooth enough as shown in Fig.3(b) (*tracing motion planning*). Thus, the tracing motion is executed by a pulling motion alone. This is the reason why we call the algorithm the pulling motion based sensing algorithm. If the environment includes another local concave as shown in Fig.3(c), however, the tip will be once away from the surface and then make contact with another part of the environment due to the rotational torque. When the probe recognizes such an additional concave area, we register $A_1$ and $B_1$ as a new pair indicating the unknown area. The sensing motion is repeated recursively for $A_1B_1$. During both *local concave point search* and *tracing motion planning*, the sensing motion may result in an infinite loop depending upon

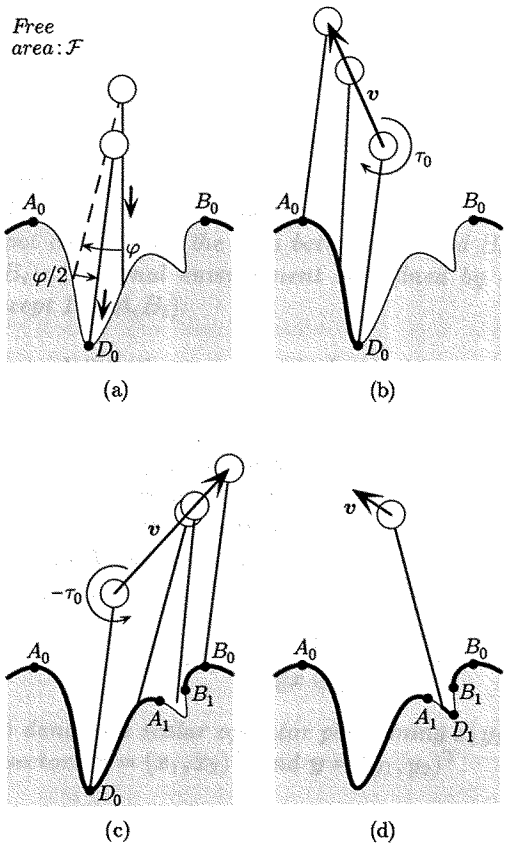


Fig. 3. Outline of the algorithm.

the environment's geometry. In order to emerge from such an infinite loop, we prepare the *infinite loop escape*, which is not always necessary but called upon request when the same contact point is detected repeatedly.

### B. Local concave point search

#### B.1 Initial pass planning

We can easily find the pass for a probe to reach the environment's surface for the unknown area $A_0B_0$. For example, the tip can surely reach the surface if the probe is inserted along a line perpendicular to $L_{A_0}^{B_0}$. For an unknown area $A_iB_i (i \neq 0)$, however, finding the pass is not always straightforward since the free area is no more clearly given like for $A_0B_0$. In this subsection, we discuss how to find the initial pass to reach the environment's surface between $A_i$ and $B_i$ and show a sufficient condition for always making the tip reach the surface between them. Before describing the sufficient condition, we provide a couple of definitions.

**Definition 1** *Consider two probe postures when the unknown area* $A_iB_i$ *is found (see Fig.4(a)).* $\mathcal{G}_i$ *is defined as the region constructed by connecting* $A_i$, $B_i$ *and each joint of the probe. If both* $A_i$ *and* $B_i$ *are detected by one probe posture,* $\mathcal{G}_i$ *is generated by rotating the probe around the tip till it makes contact with the environment as shown in Fig.5(a).*

All possible shapes for $\mathcal{G}_i$ can be classified into three

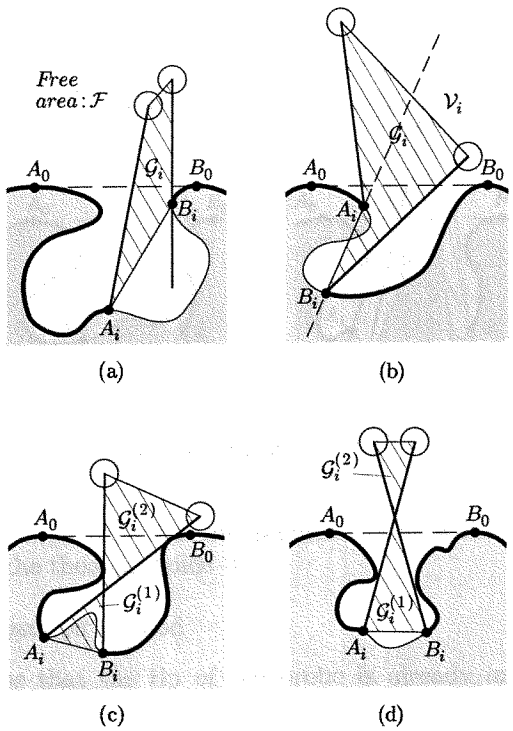


Fig. 4. Two probe postures when $A_iB_i$ is detected.

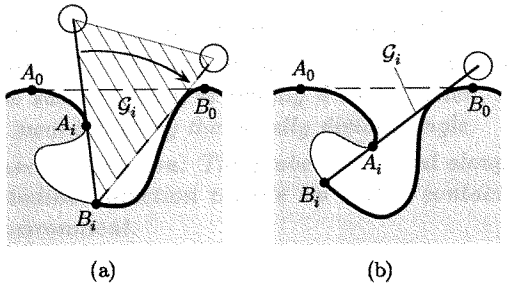


Fig. 5. An example of single probe detection.

groups, one polygon (triangle or quadrangle), two triangles (Fig.4(c) and (d)), and one line segment (Fig.5(a)), where the difference between (c) and (d) depends upon whether $L_{A_0}^{B_0}$ passes through $\mathcal{G}_i^{(1)}$ or $\mathcal{G}_i^{(2)}$. For a single probe detection as shown in Fig.5(a), $\mathcal{G}_i$ forms either a triangle or a line segment ($Area(\mathcal{G}_i) = 0$). $Area(\mathcal{G}_i) = 0$ means no more rotational degree of freedom around the tip. In other words, there exists no other pass except the current one resulting in the single probe posture as shown in Fig.5(b). Once $Area(\mathcal{G}_i) = 0$ is detected, the algorithm categorizes the $A_iB_i$ into never touching area $W_3$ and leaves from the initial pass planning. In this subsection, we temporarily assume $Area(\mathcal{G}_i) \neq 0$. Under such an assumption, there exist only two patterns for $\mathcal{G}_i$ namely, one polygon and two triangles. Since $\mathcal{G}_i$ always links with the free area $\mathcal{F}$ under assumption in III-B (the probe is long enough to ensure that the joint never enters within the unknown area), it is guaranteed that if there is an environment within $\mathcal{G}_i$, its root must be connected with $A_iB_i$. If this does not hold true, the environment in $\mathcal{G}_i$ must be an island-like-object. Under the assumption of single object (or environment), however, such a situation never appears. As for the environment classification, we give the following definitions.

**Definition 2** *For the area $A_iB_i$, internal and external environments are defined as follows:*
*$Int(A_iB_i)$: Internal environment is defined as the one whose root comes from the area between $A_i$ and $B_i$.*
*$Ext(A_iB_i)$: External environment is defined by the area $A_iB_i$ except $Int(A_iB_i)$.*

Let us now define the area $\mathcal{V}_i$ which provides another restriction for the pass.

**Definition 3** *Suppose an arbitrary point $Q$ denoted by the vector $\boldsymbol{q}$ with respect to $\Sigma_0$. Let $\boldsymbol{a}_i$ and $\boldsymbol{b}_i$ be two vectors expressing the positions $A_i$ and $B_i$ with respect to $\Sigma_0$. Define $\mathcal{V}_i$ as an assemble of $\boldsymbol{q}$ satisfying $V_i(\boldsymbol{q}) = sgn\{(\boldsymbol{a}_i - \boldsymbol{q}), (\boldsymbol{b}_i - \boldsymbol{q})\} > 0$, where $sgn(\boldsymbol{x}, \boldsymbol{y})$ is given by*

$$sgn(\boldsymbol{x}, \boldsymbol{y}) = \frac{\boldsymbol{x} \otimes \boldsymbol{y}}{\|\boldsymbol{x} \otimes \boldsymbol{y}\|} \tag{1}$$

*where, $\otimes$ denotes a scalar operator performing $x_1y_2 - x_2y_1$ for two vectors $\boldsymbol{x} = (x_1, x_2)^{\mathrm{T}}$ and $\boldsymbol{y} = (y_1, y_2)^{\mathrm{T}}$.*

Consider two half planes whose boundary line includes the line segment $A_iB_i$. By definition 3, $\mathcal{V}_i$ denotes the half plane that we can see in the right hand side when moving from $B_i$ to $A_i$. Supposing that the probe is inserted along its longitudinal direction, we now describe a sufficient condition for making the tip reach $Int(A_iB_i)$.

**Theorem 1** *A sufficient condition for making the tip reach $Int(A_iB_i)$ is to move the probe along the line passing through one point on $L_{A_0}^{B_0} \cap \mathcal{G}_i \cap \mathcal{V}_i$ and one point on $L_{A_i}^{B_i}$, where if $\mathcal{G}_i \cap \mathcal{V}_i$ is composed of two triangles, one point on $L_{A_i}^{B_i}$ is replaced by the common point for both triangles.*

**Proof :** $L_{A_0}^{B_0} \cap \mathcal{G}_i$ expresses the line segment of $L_{A_0}^{B_0}$ within $\mathcal{G}_i$. Similarly, $L_{A_0}^{B_0} \cap \mathcal{G}_i \cap \mathcal{V}_i$ denotes the line segment of $L_{A_0}^{B_0}$ within $\mathcal{G}_i \cap \mathcal{V}_i$. Note that there are two possible shapes constructed by $\mathcal{G}_i \cap \mathcal{V}_i \cap \overline{\mathcal{F}}$, one is convex (Fig.4(a), (b), (d) and Fig.5(b)) and the other is concave (Fig.4(c)).
(i) $\mathcal{G}_i \cap \mathcal{V}_i \cap \overline{\mathcal{F}}$ is a convex polygon: Assume a half-straight line starting from an arbitrary point on $L_{A_0}^{B_0} \cap \mathcal{G}_i \cap \mathcal{V}_i$ toward $L_{A_i}^{B_i}$. Since $\mathcal{G}_i \cap \mathcal{V}_i \cap \overline{\mathcal{F}}$ is convex polygon, the half-straight line comes out only from the line segment $A_iB_i$ without passing through the other line segments. Therefore, the tip comes out from $L_{A_i}^{B_i}$ or stop due to the existence of $Int(A_iB_i)$ before reaching $L_{A_i}^{B_i}$. Once the tip comes out from $L_{A_i}^{B_i}$, the only feasible case is that the tip makes contact with $Int(A_iB_i)$. In any case, the tip finally reaches on $Int(A_iB_i)$.
(ii) $\mathcal{G}_i \cap \mathcal{V}_i \cap \overline{\mathcal{F}}$ is a concave polygon: Fig.4(c) is the only example of this case. Since the polygon is composed of two triangles having the common top angle, the half-straight line starting from an arbitrary point on $L_{A_0}^{B_0} \cap \mathcal{G}_i \cap \mathcal{V}_i$ toward the common point always reaches $Int(A_iB_i)$ without com-

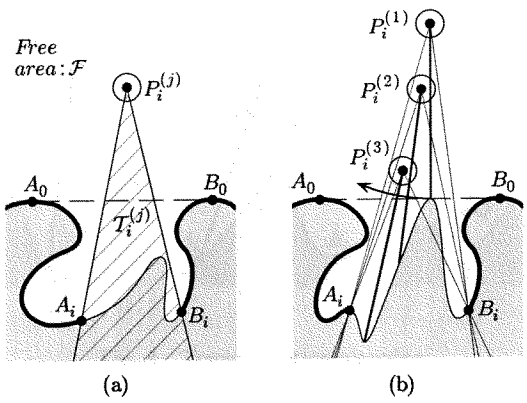


Fig. 6. Definition of $\mathcal{T}_i^{(j)}$.

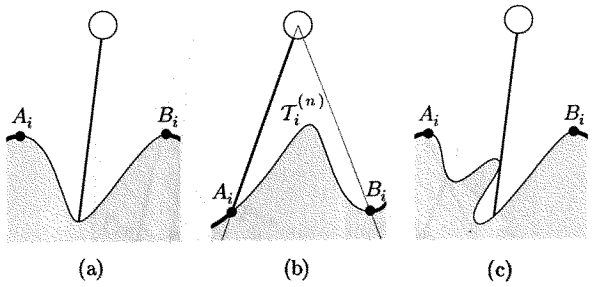


Fig. 7. Final states after bisection method: (a) Local concave point; (b) Intersection between the environment's surface and $\mathcal{T}_i^{(n)}$; (c) Multiple contacts.

ing out from the other line segment forming the polygon. Thus, the theorem holds true. ■

B.2 Bisection method

Suppose that the tip of the probe is already in contact with $Int(A_iB_i)$ by initial pass planning. Then, bisection method has the following procedure:

*(i) Swing motion: The probe is rotated around the joint until either it makes contact with an environment or it exceeds a prescribed rotational angle.*

*(ii) Dividing: The angular displacement obtained during the swing motion is equally divided. Then, the probe is swung back by the equally divided angle.*

*(iii) Inserting motion: The probe is inserted along the longitudinal direction till the tip makes contact with an environment.*

*(iv) (i) through (iii) are repeated until the probe results in one of the following states, (a) The probe loses any rotational degree of freedom around the joint, or (b) The tip converges the intersection between the environment's surface and the boundary imparted as a constraint condition.*

If and only if the probe loses any rotational degree of freedom under the single point contact at the tip, the obtained point should be at the local concave point.

**Definition 4** *Let the joint position be $P_i$. Define $\mathcal{T}_i$ as a semi-infinite region sandwiched by two lines $P_iA_i$ and $P_iB_i$.*

$\mathcal{T}_i^{(j)}$ is shown by the hatched line in Fig.6(a), where the upperscript $(j)$ denotes the value after $j$-th insertion. Now let us consider an extreme case, where the initial contact is achieved at the top of the hill as shown in Fig.6(b). The bisection method starts by swinging the probe in the left direction (or right direction). Since the probe always goes into the safety area $\mathcal{F}$ in this particular case, the probe will not make contact with the environment any more. Therefore, we need a boundary, such that we can stop the swing motion. For this purpose, $\mathcal{T}_i^{(j)}$ provides a reasonable boundary.

**Theorem 2** *Suppose that an initial contact with $Int(A_iB_i)$ is already completed. A sufficient condition for making the tip finally converge on $Int(A_iB_i)$ is to execute bisection method such that the tip may not come out from the boundary of $\mathcal{T}_i^{(j)} \cap \mathcal{V}_i \cap \mathcal{G}_i$ except the line segment $A_iB_i$.*

**Proof :** Since there is no $Ext(A_iB_i)$ within $\mathcal{T}_i^{(j)} \cap \mathcal{V}_i \cap \mathcal{G}_i$, the tip comes out from $L_{A_i}^{B_i}$ or stops due to the existence of $Int(A_iB_i)$ before reaching $L_{A_i}^{B_i}$. Once the tip comes out from $L_{A_i}^{B_i}$, the only feasible case is that it makes contact with $Int(A_iB_i)$. In any case, the tip finally reaches on $Int(A_iB_i)$. ■

*C. Tracing motion planning*

C.1 Realization of the pulling motion

When the *local concave search* comes to the end, there are basically two possible cases as shown in Fig.7, namely, the tip finally reaches a local concave point (a), and it stops at a non-local concave point ((b) and (c)). In Fig.7(b) and (c), the tip stops due to the boundary constraint (b) and due to multiple contacts (c), respectively.

**Definition 5** *$Y_1$ denotes the final contact mode where $Y_1 = 1$ means that only the tip makes contact with the environment, and $Y_1 = 2$ means multiple contacts at the tip and other points. $Y_2$ denotes the rotational constraint, where $Y_2 = 0$, 1 and $-1$ are full constraint, single constraint for the clockwise direction, and single constraint for the counter clockwise direction, respectively.*

**Definition 6** *Define $\mathcal{K}_1$ as an assemble of $\boldsymbol{v}$ satisfying $\boldsymbol{v}^{\mathrm{T}}\boldsymbol{t}^* < 0$, where $\boldsymbol{v}$ and $\boldsymbol{t}$ are vectors expressing the moving direction of the joint, and the longitudinal direction of the probe, respectively, and $*$ denotes the value just after the bisection method is completed. Also, define $\mathcal{K}_2$ as an assemble of $\boldsymbol{v}$ satisfying $sgn(\boldsymbol{v}, \boldsymbol{t}^*) < 0$.*

**Definition 7** *$Face(right) = ON$ (or $Face(left) = ON$ or $Face(tip) = ON$) means that a part of right side (or left side or tip) of the probe makes contact with an environment.*

Based on the definition 5, the three cases (a), (b), and

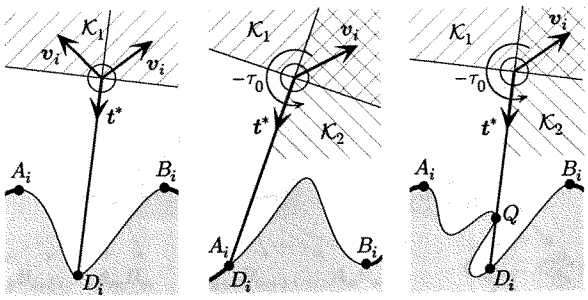


Fig. 8. Tracing motion planning.

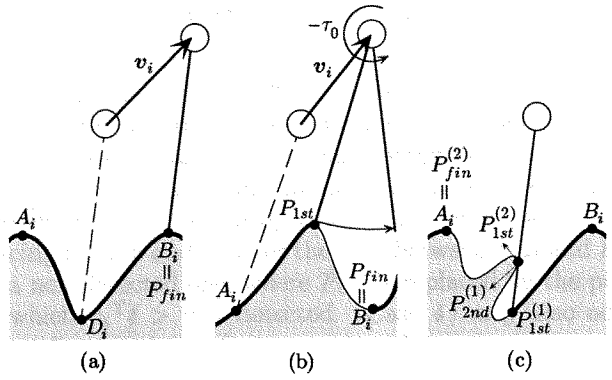


Fig. 9. Realization of tracing motion.

(c) can be classified by $(Y_1, Y_2) = (1,0)$, $(Y_1, Y_2) = (1, -1 \text{ or } 1)$, $(Y_1, Y_2) = (2,0)$, respectively.

**Theorem 3** *A sufficient condition for achieving a pulling motion based tracing is to determine the moving direction of the joint and the joint torque, such that* $v_i \in \mathcal{K}$ *and*

$$\tau = \tau_0 sgn(v_i, t^*) \tag{2}$$

*where* $\tau_0 (> 0)$ *is the reference torque and the positive direction of* $\tau$ *is chosen in the clockwise direction, and* $\mathcal{K}$ *is given below.*

**(A)** : *If* $(Y_1, Y_2) = (1,0)$, $\mathcal{K} = \mathcal{K}_1$ *(see Fig.8(a)).*

**(B)** : *If* $(Y_1, Y_2) = (1,-1)$, $\mathcal{K} = \mathcal{K}_1 \cap \mathcal{K}_2$ *(see Fig.8(b)).*

**(C)** : *If* $(Y_1, Y_2) = (1,1)$, $\mathcal{K} = \mathcal{K}_1 \cap \overline{\mathcal{K}_2}$.

**(D)** : *If* $(Y_1, Y_2) = (2,0)$ *and* $Face(left) = ON$, $\mathcal{K} = \mathcal{K}_1 \cap \mathcal{K}_2$ *(see Fig.8(c)).*

**(E)** : *If* $(Y_1, Y_2) = (2,0)$ *and* $Face(right) = ON$, $\mathcal{K} = \mathcal{K}_1 \cap \overline{\mathcal{K}_2}$.

**Proof :** We omit the proof due to the paper space limitation. ■

C.2 All possible cases during tracing motion

Tracing motion is continued until the tip successfully traces from the initial point $D_i$ to $A_i$ (or $B_i$) as shown in Fig.9(a). However, the contact between the probe and the environment is not always guaranteed during the tracing motion. For example, the tip may be away from the environment at the top of the hill during the tracing motion from $A_i$ to $B_i$, as shown in Fig.9(b).

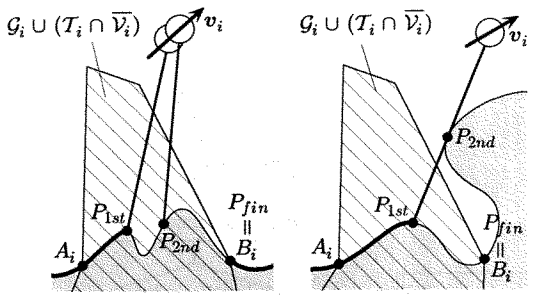


Fig. 10. $P_{2nd}$ detected on $Int(A_iB_i)$ or $Ext(A_iB_i)$.

**Definition 8** *Let* $P_{fin}$ *be the destination point for a tracing motion. We choose* $P_{fin} = A_i$ *for* $sgn(v_i, t^*) > 0$ *or* $P_{fin} = B_i$ *for* $sgn(v_i, t^*) < 0$.

We stop the tracing motion when a part of the probe reaches $P_{fin}$. During the tracing motion, however, there might appear a contact point jump due to the surface geometry. For such a contact point jump, we define two points $P_{1st}$ and $P_{2nd}$ as follows.

**Definition 9** *Let* $P_{1st}$ *and* $P_{2nd}$ *be the contact points just before and after a contact point jump, respectively. In case of a single probe detection, the point closer to the tip is chosen as* $P_{1st}$.

All possible cases during a tracing motion can be classified as follows:

〈Case 1〉 All contact points are continuously detected by the probe tip for the designated area.

〈Case 2〉 At least, one contact point jump appears.

〈Case 3〉 $v_i{}^{\mathrm{T}} t > 0$ is detected.

〈Case 4〉 The joint loses the moving degree of freedom in the direction given by $v_i$.

Since 〈Case 1〉 means that the designated unknown area $Int(A_iB_i)$ becomes known, we can simply categorize such an area into $W$. For one of the three other cases, however, we have to memorize a part of $Int(A_iB_i)$ as a further non-detected area. Let us now consider which points we should register for 〈Case 2〉 , 〈Case 3〉 and 〈Case 4〉 . For this purpose, 〈Case 2〉 is further classified into the following three cases.

〈Case 2-1〉 $P_{2nd}$ exists on $Int(A_iB_i)$.

〈Case 2-2〉 $P_{2nd}$ exists on $Ext(A_iB_i)$.

〈Case 2-3〉 $P_{2nd}$ does not exist within $\overline{\mathcal{F}}$.

〈Case 2-1〉 or 〈Case 2-2〉 is distinguished by checking whether $P_{2nd} \in \mathcal{G}_i \cup (\mathcal{T}_i \cap \overline{\mathcal{V}_i})$ or $P_{2nd} \in \overline{\mathcal{G}_i} \cap (\overline{\mathcal{T}_i} \cup \mathcal{V}_i)$, respectively, as shown in Fig.10(a) and (b). 〈Case 2-3〉 happens when the probe enter $\mathcal{F}$ without any contact. In 〈Case 2-1〉 , the area between $P_{1st}$ and $P_{2nd}$ is registered as a non-detected area and then the tracing motion is continued for the remaining non-traced area. In both

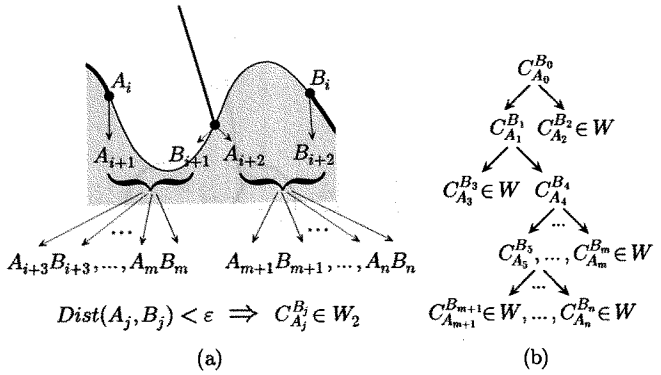


Fig. 11. Infinite loop escape.

〈Case 2-2〉 and 〈Case 2-3〉 , we stop any further tracing motion and register the area between $P_{1st}$ and $P_{fin}$ as a non-detected area. 〈Case 3〉 may occur because the condition realizing a pulling motion is satisfied only at the starting position. Once ${\boldsymbol{v}_i}^{\mathrm{T}}\boldsymbol{t} > 0$ is detected, we stop the tracing motion and register the area between $P_{1st}$ and $P_{fin}$ as a non-detected one, where $P_{1st}$ is replaced by the point in which ${\boldsymbol{v}_i}^{\mathrm{T}}\boldsymbol{t} > 0$ is detected. 〈Case 4〉 may also occur depending on the surface geometry, the probe posture and the moving direction of the probe. Once the probe loses the degree of freedom in the direction $\boldsymbol{v}_i$, we stop the tracing motion and register the area between $P_{1st}$ and $P_{fin}$ as a non-detected one, where $P_{1st}$ is replaced by the point in which the probe loses the degree of freedom. In case of Fig.8(c), according to the theorem 3, the tracing motion is not executed in the direction from $D_i$ to $A_i$. In such a situation, we register $(P_{1st}^{(1)}, P_{2nd}^{(1)})$ and $(P_{1st}^{(2)}, P_{fin}^{(2)})$ as non-detected areas after regarding $(P_{1st}^{(1)}, P_{2nd}^{(1)}) = (D_i, Q)$ and $(P_{1st}^{(2)}, P_{fin}^{(2)}) = (Q, A_i)$ as shown in Fig.9(c). The non-detected area, such as $(P_{1st}, P_{2nd})$ have to be finally stored into $(A_j, B_j)$ for executing the program recursively.

〈Rule to determine $(A_j, B_j)$〉
(i) In case of $P_{fin} = A_i$: $(A_j, B_j) = (P_{2nd}$ or $P_{fin}, P_{1st})$.
(ii) In case of $P_{fin} = B_i$: $(A_j, B_j) = (P_{1st}, P_{2nd}$ or $P_{fin})$.

### *D. Infinite loop escape*

There might be a particular state in which the tip can find the same point repeatedly during the *local concave point search* and the *tracing motion planning*. Every algorithm has a possibility resulting in such an infinite mode. In order to avoid such an undesirable mode, we prepare the *infinite loop escape*, where the probe temporarily searches a new contact point by utilizing the same way taken in the initial pass planning. Since the initial pass planning ensures to find a new contact point between $A_iB_i$, we can separate the area $A_iB_i$ into two new areas $A_{i+1}B_{i+1}$ and $A_{i+2}B_{i+2}$, as shown in Fig.11(a). After dividing the area, we leave from the *infinite loop escape* and come back to the normal mode given by *local concave point search* and *tracing motion planning*. Now, assume that an infinite mode appears every time after initial pass planning motion. In such an extreme case, $A_{i+1}B_{i+1}$ (or $A_{i+2}B_{i+2}$) is further separated into two unknown areas $A_{i+3}B_{i+3}$ and $A_{i+4}B_{i+4}$, and so forth, as shown in Fig.11(a). For every newly divided area, if $Dist(A_j, B_j) < \varepsilon$ is satisfied, any further separation between $A_j$ and $B_j$ is stopped and $C_{A_j}^{B_j} \in W_2$ is assigned. This implies that the algorithm brings the environment's shape in relief even when an infinite loop occurs continuously.

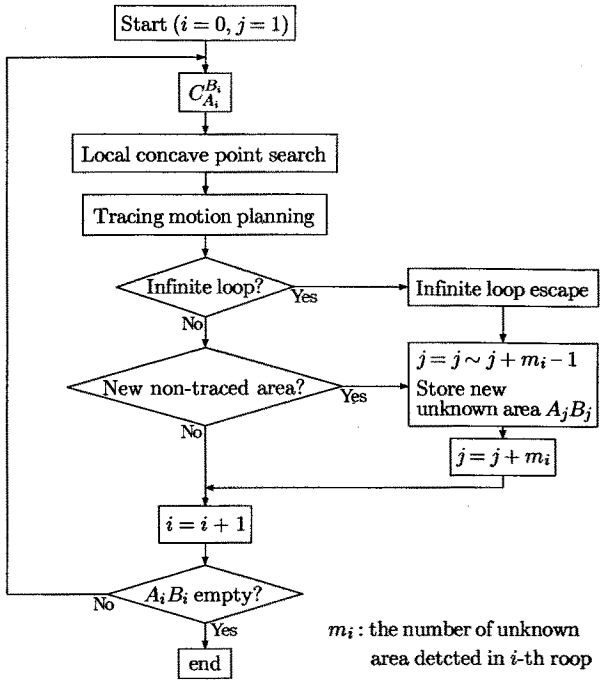


Fig. 12. Flowchart.

## V. Simulation

Fig.12 shows the overall flowchart of the proposed algorithm. The sensing motion continues until every unknown area is assigned to $W = \cup_{i=1}^{3} W_i$. Fig.13 shows a simulation result, where the real and the dotted lines denote the known and the unknown areas, respectively, and the line segment passing through the joint expresses the moving direction of the joint, which is determined by the sufficient condition given by theorem 3. From this simulation result, it can be understood that the unknown area gradually decreases and finally disappears except the particular area which the probe cannot reach and touch.

## VI. Experiment

The experiment is also done by utilizing the planar type three d.o.f wire driven robot whose end is connected with a probe. The robot has a joint position sensor and a specially designed torque sensor in each joint. Although the probe has no sensing capability by itself, both torque and position sensor outputs enable us to localize the contact point between the probe and the environment. In order to always ensure the single point contact, a simple concave environment is prepared for the experiment. Fig.14 shows

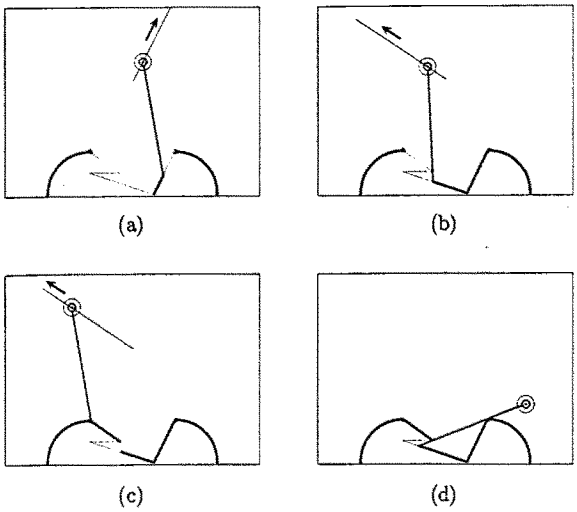


Fig. 13. Simulation result.

a set of photos during the experiment, where (a), (b) and (c) illustrate the bisection method, the left tracing motion and the right tracing motion, respectively. The LED with the flashing rate of 5Hz is equipped with the tip of the probe so that we can clearly see the trajectory of the tip, while executing both the bisection method and the tracing motion.

## VII. Conclusions

A tactile sensing algorithm for detecting the concave surface has been proposed. We have shown sufficient conditions for the probe tip to reach the designated unknown area and to converge within the area after bisection method. We have also found sufficient conditions for avoiding any pushing motion at the beginning of a tracing motion. In our next step, we will extend the pulling-motion-based tactile sensing into a 3D concave environment. Since tracing every area for a 3D environment is not as feasible as that in a 2D one, the parametrized local surface function [18] may be a useful tool for expressing the surface shape with respect to a local contact frame. We believe, however, that the concept of the pulling-motion-based tracing should be still included even in the algorithm for surface sensing of a 3D environment.

Finally, we would like to express our sincere gratitude to Mr. N. Thaiprasert for his cooperation in the experiment.

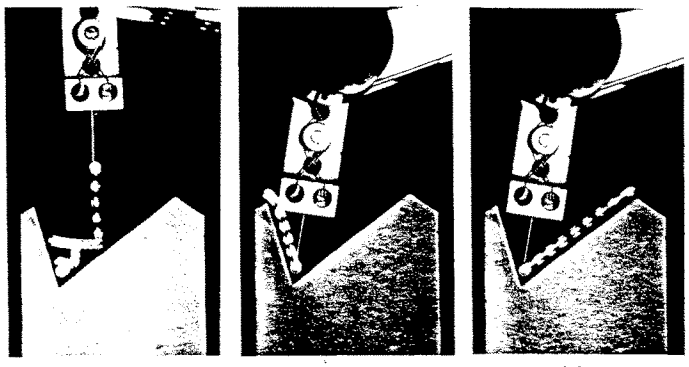


Fig. 14. An example of experiment: (a) Bisection method; (b) Left tracing motion; (c) Right tracing motion.

## References

[1] Dario, P. and G. Buttazzo: An anthropomorphic robot finger for investigating artificial tactile perception, Int J. Robotics Research, vol.6, no.3, pp25–48, 1987.

[2] Fearing, R. S. and T. O. Binford: Using a cylindrical tactile sensor for determining curvature, Proc. of the IEEE Int. Conf. on Robotics and Automation, Philadelphia, pp765–771, 1988.

[3] Maekawa, H., K. Tanie, K. Komoriya, M. Kaneko, C. Horiguchi, and T. Sugawara: Development of a finger-shaped tactile sensor and its evaluation by active touch, Proc. of the IEEE Int. Conf. on Robotics and Automation, Nice, pp1327, 1992.

[4] Salisbury, J. K.: Interpretation of contact geometries from force measurements, Proc. of the 1st Int. Symp. on Robotics Research, 1984.

[5] Brock, D.L. and S.Chiu: Environment perception of an articulated robot hand using contact sensors, Proc. of the IEEE Int. Conf. on Robotics and Automation, Raleigh, pp89–96, 1987.

[6] Kaneko, M., and K. Honkawa: Compliant motion based active sensing by robotic fingers, Preprints of the 4th IFAC Symp. on Robot Control, Capri, pp137–142, 1994.

[7] Allen, P. and K. S. Roberts: Haptic object recognition using a multi-fingered dexterous hand, Proc. of the IEEE Int. Conf. on Robotics and Automation, pp342–347, 1989.

[8] Bajcsy, R.: "What can we learn from one finger experiments?", Proc. of the 1st Int. Symp on Robotics Research, pp509–527, 1984.

[9] Bicchi, A., Salisbury J. K. and D. J. Brock: Contact sensing from force measurements, Int. J. of Robotics Research, vol.12, no.3, 1993

[10] Bays, J. S. : Tactile shape sensing via single- and multi-fingered hands, Proc. of the IEEE Int. Conf. on Robotics and Automation, PP 290–295, 1989.

[11] Caselli, S., C. Magnanini, F. Zanichelli, and E. Caraffi: Efficient exploration and recognition of convex objects based on haptic perception, Proc. of the IEEE Int. Conf. on Robotics and Automation, PP 3508–3513, 1996.

[12] Gaston, P. C., and T. Lozano-Perez: Tactile recognition and localization using object models, The case of polyhedra on a plane, MIT Artificial Intelligence Lab. Memo, no.705, 1983.

[13] Grimson, W. E. L. and T. Lozano-Perez: Model based recognition and localization from sparse three dimensional sensory data, AI Memo 738, MIT, AI Laboratory, Cambridge, MA, 1983.

[14] Cole, R., and C. K. Yap: Shape from probing, J. of Algorithms 8, pp19–38, 1987.

[15] Russell, R. A. : Using tactile whiskers to measure surface contours, Proc. of the 1992 IEEE Int. Conf. on Robotics and Automation, pp1295–1300, 1992.

[16] Tsujimura, T. and T. Yabuta: Object detection by tactile sensing method employing force/moment information, IEEE Trans. on Robotics and Automation, vol.5, no.4, pp444–450, 1988.

[17] Roberts, K. S. : Robot active touch exploration, Proc. of the IEEE Int. Conf. on Robotics and Automation, PP 980–985, 1990.

[18] Chen, N., R. Rink, and H. Zhang: Local object shape from tactile sensing, Proc. of the IEEE Int. Conf. on Robotics and Automation, PP 3496–3501, 1996.

[19] Boissonnat, J. D. and M. Yvinec: Probing a scene of non-convex polyhedra, Algorithmica, vol.8, pp321–342, 1992